ISSN: 2319-5967
ISO 9001:2008 Certified
International Journal of Engineering Science and Innovative Technology (IJESIT)
Volume 3, Issue 1, January 2014

Neural Network based FACTS Controller for Enhancement of Power System Dynamic Stability

Mithilesh Das, Dr. Ramesh Kumar, Rajib Kumar Mandal

Abstract: ***This paper presents a Hybrid method for power system dynamic stability enhancement. Hybrid method consists of Interline Power flow Controller with RBFNN and Lead- Lag as a supplementary Controller. Here for Power system dynamic stability prospect low power frequency oscillation has been kept into the consideration. For modelling purposes SMIB System is being used and also for analysis purposes Phillip Heffron model of equivalent SMIB System has been used. Matlab Simulation provides the time domain analysis of the System.***

Keywords: **IPFC, RBFNN, SMIB, Lead-Lag Controller and Phillip Heffron Model.**

I. INTRODUCTION

Power systems are subjected to low frequency disturbances that might cause loss of synchronism and an eventual breakdown of entire system. The oscillations, which are typically in the frequency range of 0.2 to 3.0 Hz, might be excited by the disturbances in the system or, in some cases, might even build up spontaneously. These oscillations limit the power transmission capability of a network and, sometimes, even cause a loss of synchronism and an eventual breakdown of the entire system. For this purpose, Power system stabilizers (PSS) are used to generate supplementary control signals for the excitation system in order to damp these low frequency power system oscillations.

The use of power system stabilizers has become popular in the form of POD controller. By the virtue of advancement in Technology FACTS controller replaces the Conventional Power System Stabilizer [1]. In this work, we deal with damping out the low power frequency oscillations. Small deviation (0.01 p.u.) in the mechanical power (Mechanical Torque) has been taken into consideration for the purposes of analysis. A model of Power System named as "Phillip- Heffron Model" has been implemented for the time domain analysis. An Interline Power Flow Controller (IPFC) has been used here as a FACTS controller. A Radial Basis Function Neural Network (RBFNN) controller and Lead- Lag controller have been used as supplementary controller for the FACTS controller. Result obtained from RBFNN based FACTS controller and Lead-Lag based FACTS controller are compared.

II. POWER SYSTEM MODELLING

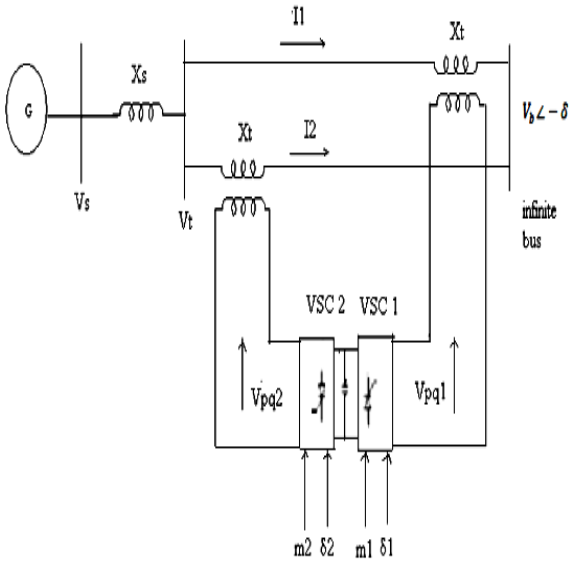

Fig.1: Single Machine Infinite Bus installed with IPFC

ISSN: 2319-5967
ISO 9001:2008 Certified
International Journal of Engineering Science and Innovative Technology (IJESIT)
Volume 3, Issue 1, January 2014

Fig. 1 shows a single machine infinite bus installed with Interline Power Flow Controller [3] which consist of two, three phase GTO based voltage source converters, each providing a series compensation for the two lines is incorporated in the system. VSCs are connected to the transmission line through their series coupling transformers. Hence the configuration allows the control of real and reactive power flow of line 1. Here m_1 & m_2 are the amplitude modulation ratio and δ_1 & $\delta 2$ are phase angle of the control signal of each VSCs respectively, which are the input control signals of IPFC. V_s, V_b, V_{pq1}, and V_{pq2} are the terminal voltage of generator, voltage of infinite bus, and voltage of VSCs respectively.

Linearized model of SMIB installed with IPFC [2] can be represented as:

$$\Delta\dot{\delta} = \omega_0\Delta\omega$$
$$\Delta\dot{\omega} = (-\Delta P_e - D\Delta\omega)/M$$
$$\Delta\dot{E}_q^{'} = \left(-\Delta E_q + \Delta E_{fd}\right)/T_{d0}^{'}$$
$$\Delta\dot{E}_{fd} = -\frac{1}{T_A}\Delta E_{fd} + \frac{K_A}{T_A}\Delta V_t \quad -----(1)$$

Where,

$$\Delta P_e = K_1\Delta\delta + K_2\Delta E_q^{'} + K_{pv}\Delta V_{DC} + K_{pm_1}\Delta m_1 + K_{p\delta_1}\Delta\delta_1 + K_{pm_2}\Delta m_2 + K_{p\delta_2}\Delta\delta_2 \quad --------(2)$$
$$\Delta E_q^{'} = K_4\Delta\delta + K_3\Delta E_q^{'} + K_{qv}\Delta V_{DC} + K_{qm_1}\Delta m_1 + K_{q\delta_1}\Delta\delta_1 + K_{qm_2}\Delta m_2 + K_{q\delta_2}\Delta\delta_2 \quad --------(3)$$
$$\Delta V_t = K_5\Delta\delta + K_6\Delta E_q^{'} + K_{vv}\Delta V_{DC} + K_{vm_1}\Delta m_1 + K_{v\delta_1}\Delta\delta_1 + K_{vm_2}\Delta m_2 + K_{v\delta_2}\Delta\delta_2 \quad --------(4)$$
$$\Delta\dot{V}_{DC} = K_7\Delta\delta + K_8\Delta E_q^{'} + K_9\Delta V_{DC} + K_{cm_1}\Delta m_1 + K_{c\delta_1}\Delta\delta_1 + K_{cm_2}\Delta m_2 + K_{c\delta_2}\Delta\delta_2 \quad --------(5)$$

By substituting (2-5) with (1),we can obtain the state variable equation of SMIB Power system installed with IPFC:

$$\begin{bmatrix} \Delta\dot{\delta} \\ \Delta\dot{\omega} \\ \Delta\dot{E}_q^{'} \\ \Delta\dot{E}_{fd} \\ \Delta\dot{V}_{DC} \end{bmatrix} = \begin{bmatrix} 0 & \omega_0 & 0 & 0 & 0 \\ -\frac{K_1}{M} & -\frac{D}{M} & -\frac{K_2}{M} & 0 & -\frac{K_{pv}}{M} \\ -\frac{K_4}{T_{d0}^{'}} & 0 & -\frac{K_3}{T_{d0}^{'}} & \frac{1}{T_{d0}^{'}} & -\frac{K_{qv}}{T_{d0}^{'}} \\ -\frac{K_A K_5}{T_A} & 0 & -\frac{K_A K_6}{T_A} & -\frac{1}{T_A} & -\frac{K_A K_{vv}}{T_A} \\ K_7 & & K_8 & 0 & K_9 \end{bmatrix} \begin{bmatrix} \Delta\delta \\ \Delta\omega \\ \Delta E_q^{'} \\ \Delta E_{fd} \\ \Delta V_{DC} \end{bmatrix} + \begin{bmatrix} 0 & 0 & 0 & 0 \\ -\frac{K_{pm_1}}{M} & -\frac{K_{p\delta_1}}{M} & -\frac{K_{pm_2}}{M} & -\frac{K_{p\delta_2}}{M} \\ -\frac{K_{qm_1}}{T_{d0}^{'}} & -\frac{K_{q\delta_1}}{T_{d0}^{'}} & -\frac{K_{qm_2}}{T_{d0}^{'}} & -\frac{K_{q\delta_2}}{T_{d0}^{'}} \\ -\frac{K_{vm_1}}{T_A} & -\frac{K_{v\delta_1}}{T_A} & -\frac{K_{vm_2}}{T_A} & -\frac{K_{v\delta_2}}{T_A} \\ K_{cm_1} & K_{c\delta_1} & K_{cm_2} & K_{c\delta_2} \end{bmatrix} \begin{bmatrix} \Delta m_1 \\ \Delta\delta_1 \\ \Delta m_2 \\ \Delta\delta_2 \end{bmatrix} \quad -(6)$$

The PH model of the corresponding linearized model is shown in **fig. 2** [3]. In this fig, there are so many constants. These constants are functions of the system parameters and initial operating condition.
The controlled vector u is defined as:

$$\Delta u = [\Delta m_1 \quad \Delta\delta_1 \quad \Delta m_2 \quad \Delta\delta_2]^T$$

Where Δm_1, $\Delta\delta_1$, Δm_2, $\Delta\delta_2$ represent the linearization of the input control signals of the IPFC. Under this work only one input control signal is taken into consideration at a time for the analysis purposes, viz either we take $\Delta U = \Delta m_1$ or $\Delta U = \Delta\delta_1$ $\Delta U = \Delta m_2$ or $\Delta U = \Delta\delta_2$. And K_p, K_q, K_v and K_c are the row vectors defined as:

$$K_p = [K_{pm_1} \quad K_{p\delta_1} \quad K_{pm_2} \quad K_{p\delta_2}]$$
$$K_q = [K_{qm_1} \quad K_{q\delta_1} \quad K_{qm_2} \quad K_{q\delta_2}] \quad -------(7)$$
$$K_v = [K_{vm_1} \quad K_{v\delta_1} \quad K_{vm_2} \quad K_{v\delta_2}]$$

ISSN: 2319-5967
ISO 9001:2008 Certified
International Journal of Engineering Science and Innovative Technology (IJESIT)
Volume 3, Issue 1, January 2014

$K_c = [K_{cm_1} \quad K_{c\delta_1} \quad K_{cm_2} \quad K_{c\delta_2}]$

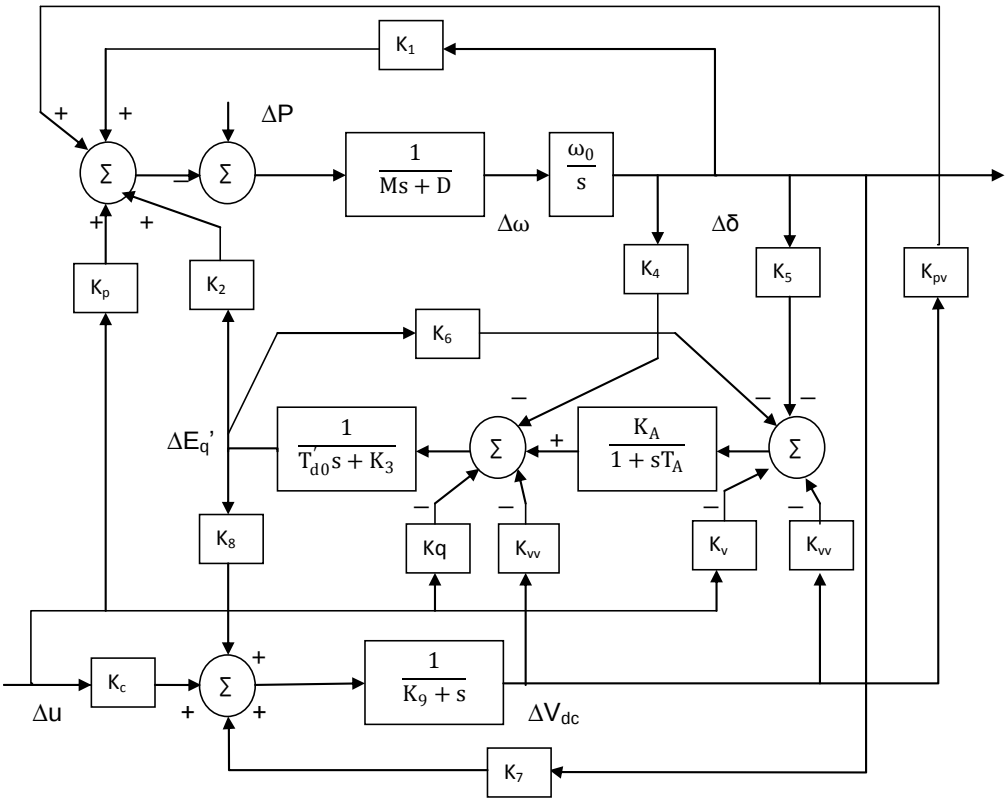

Fig. 2 : PH model of SMIB system installed with IPFC

III. DESIGN OF DAMPING CONTROLLER

Damping Controllers are designed to produce an electrical torque in phase with the speed deviation that damp out the power system oscillations. For IPFC as damping controller, there is a requirement of supplementary damping controller. RBFNN and Lead- Lag Controller have been used as supplementary Controller and their responses are compared. In this supplementary controller, either Δω or Δδ is taken as input.

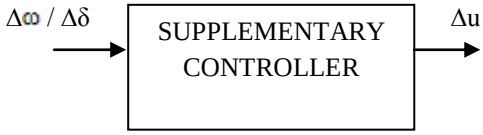

Fig. 3: Block diagram of Supplementary controller

A. Lead Lag Controller

To get fast response and good steady-state accuracy, a lead-lag controller is used. It also increases the low frequency gain and system bandwidth, making the system response fast. In general, the phase lead portion of this compensator provides large bandwidth and hence shorter rise time and settling time, while the phase lag portion provides the major damping of the system. In the lead-lag controller, phase lead and lag occur at different frequency regions. The phase lag occurs in a low frequency regions. The phase lag occurs in a low frequency region, whereas phase lead occurs in a high frequency region.

ISSN: 2319-5967
ISO 9001:2008 Certified
International Journal of Engineering Science and Innovative Technology (IJESIT)
Volume 3, Issue 1, January 2014

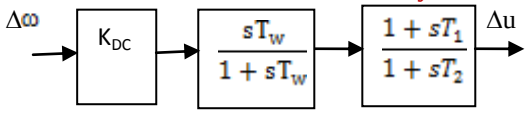

Fig. 4: structure of lead lag as supplementary controller

Steps for calculation of supplementary controller parameter:

Computation of natural frequency of oscillation ω_n by using relation

$$\omega_n = \sqrt{\frac{K_1 \omega_0}{M}}$$

K_1 is the constant of model, computed for operating condition and system parameters.
ω_0 is frequency of operating condition (rad/sec)
ω_n is natural frequency of oscillation (rad/sec)

Computation of ∟GEPA (phase angle between Δu and ΔP) at s=jω_n

Design of Phase lead lag compensator: the phase lead/lag compensator is designed to provide the required degree of phase compensation. For 100% compensation,

∟$G_c(j\omega_n)$+∟GEPA(jω_n)=0

Assuming one lead-lag network at $T_1=\propto T_2$, the transfer function becomes, $G_c(s) = \frac{1+s\propto T_2}{1+sT_2}$

Where $\alpha = \frac{1+\sin\gamma}{1-\sin\gamma}$ $\quad T_2 = \frac{1}{\omega_n\sqrt{\alpha}}$

Computation of optimum gain K_{DC}: The value of gain setting to achieve the required amount damping torque D_{IPFC} can be provided by IPFC supplementary damping controller. The signal washout is the high pass filter that prevents steady changes in the speed from modifying the IPFC input parameter. The value of the washout time constant T_w should be high enough to allow signals associated with oscillations in rotor speed to pass unchanged.Tw is not yet critical, may range from 1s to 20s.

B. Radial Basis Function Neural Network Controller

An RBF is a function which has in-built distance criterion with respect to a center [4] . A typical RBF neural network consists of three layers (input, hidden, output). The activation of a hidden neuron is determined in two steps:

First- computing the distance (usually by using the Euclidean norm) between the input vector and center C_i that represents the i^{th} hidden neuron.

Then a function h that is usually bell shaped is applied, using the obtained distance to get the final activation of the hidden neuron. In our case the well known Gaussian function G(x).

$$G(x) = exp\left(\frac{|x - C_i|^2}{2\sigma^2}\right)$$

is used. The parameter σ is called unit width. All the widths in the network are fixed to the same value σ and these result in a simpler training strategy. The activation of a neuron in the output layer is determined by a linear combination of the fixed nonlinear basis functions, i.e.

$$F(x) = \omega_0 + \sum_{i=1}^{M} \omega_i \emptyset_i(x)$$

Where $\emptyset_i = G(|x - C_i|)$ and ω_i are the adjustable weights that link the output node with the appropriate hidden neurons and ω_0 is the biasing weight. These weights in the output layer can then be learnt using the least-squares method. Since a fixed center corresponds to a given regress in a linear regression model, the selection of RBF centres can be regarded as a problem of subset selection. The orthogonal least squares (OLS) method is employed as a forward selection procedure that constructs RBF networks in a rational way. The algorithm chooses appropriate RBF centers one by one from training data points until a satisfactory network is obtained. Each selected center minimizes the increment to the explained variance of

ISSN: 2319-5967
ISO 9001:2008 Certified
International Journal of Engineering Science and Innovative Technology (IJESIT)
Volume 3, Issue 1, January 2014

the desired output, and so ill conditioning problems occurring frequently in random selection of centers can automatically be avoided. In contrast to most learning algorithms, which can only work if a fixed network structure has first been specified, the OLS algorithm is a structural identification technique, where the centers and estimates of the corresponding weights can be simultaneously determined in a very efficient manner during learning. OLS learning procedure generally produces an RBF network smaller than a randomly selected RBF network. Due to its linear computational procedure at the output layer, the RBF takes less training time compared to its back propagation counterpart.

A major drawback of this method is associated with the input space dimensionality. For large number of input units, the number of radial basis functions required, can become excessive. If too many centers are used, the large number of parameters available in the regression procedure will cause the network to be over sensitive to the details of the particular training set and result in poor generalization performance (over fit). So the data compression through vector quantization technique has improved the efficiency of RBF model

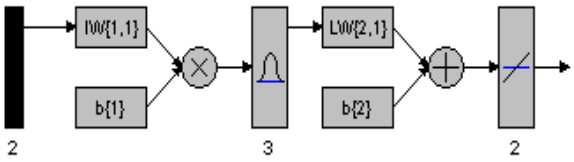

Fig. 5: Block diagram of RBFNN for fewer neurons

Here for simulink block creation sum of square of errors (SSE) function is used.

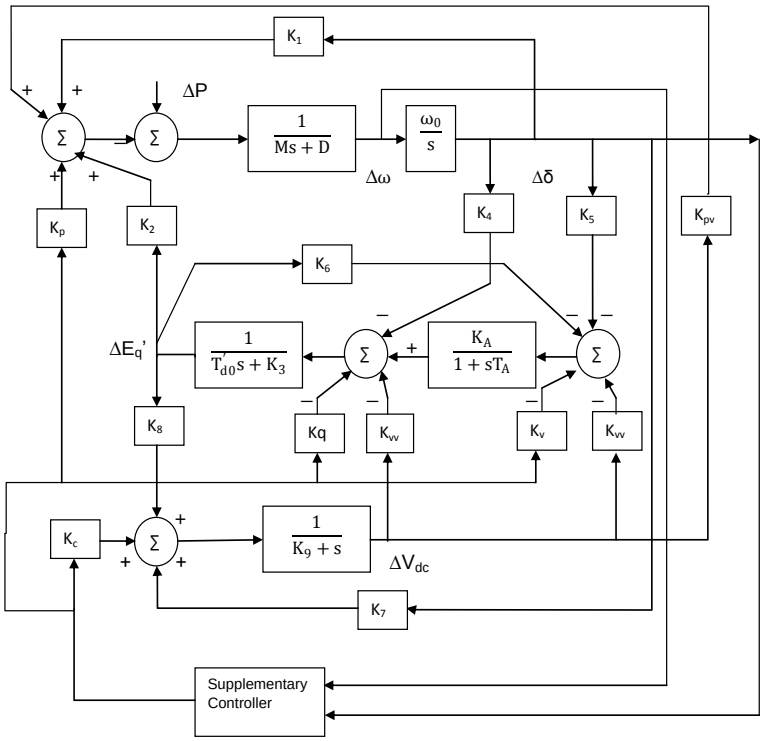

Fig. 6: PH Model of SMIB with IPFC and RBFNN/Lead-Lag Controller

IV. SIMULATION AND RESULT

To analyse the performance of IPFC controller simulation work done on the fig. 6 [4]. All the simulation being for a step change (i.e 0.01 p.u.) in mechanical power. All the constants values are mentioned in the Appendix. Simulation work is divided in three parts:

ISSN: 2319-5967
ISO 9001:2008 Certified
International Journal of Engineering Science and Innovative Technology (IJESIT)
Volume 3, Issue 1, January 2014

1. Without any supplementary controller
2. With Lead-Lag controller and
3. With RBFNN controller

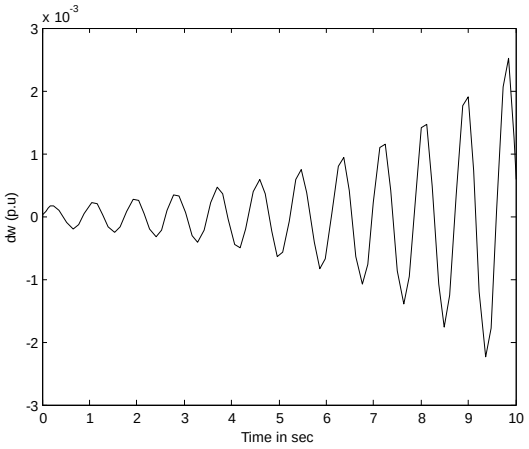

Fig. 7: Response of speed deviation (Δω) without any supplementary controller

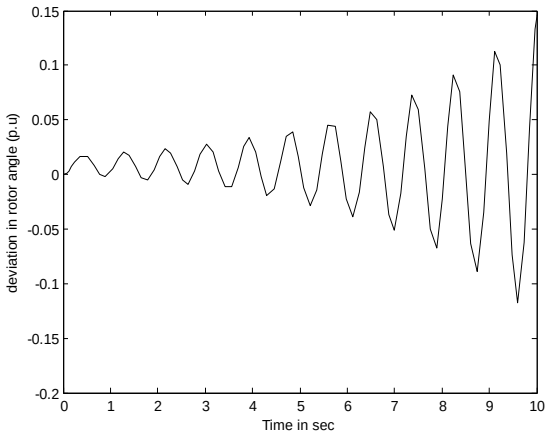

Fig. 8: Response of Rotor angle deviation (Δδ) without any supplementary

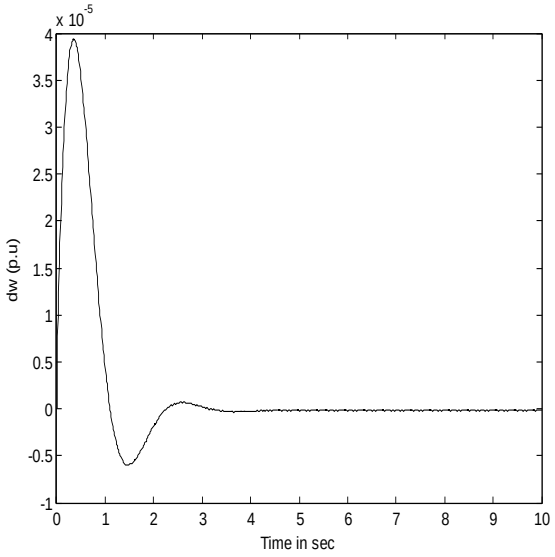

Fig. 9: Response of speed deviation (Δω) for m_1 of IPFC controller with Lead-Lag Controller

ISSN: 2319-5967
ISO 9001:2008 Certified
International Journal of Engineering Science and Innovative Technology (IJESIT)
Volume 3, Issue 1, January 2014

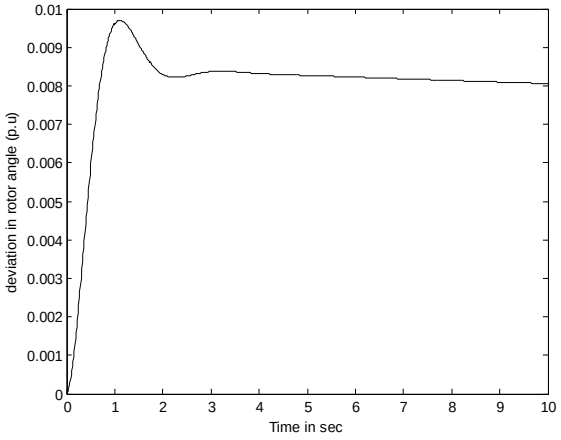

Fig. 10: Response of Rotor angle deviation (Δδ) for m_1 of IPFC controller with Lead-Lag Controller

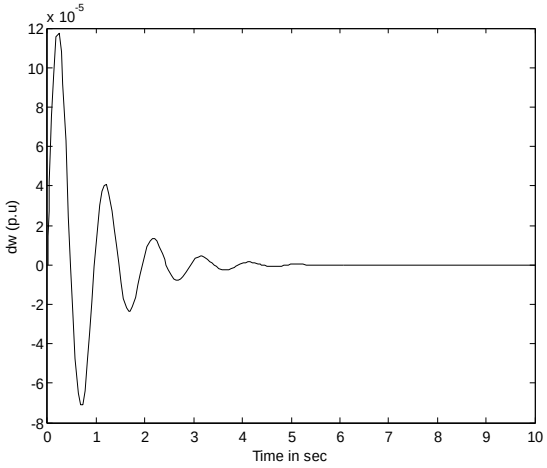

Fig. 11: Response of speed deviation (Δω) for $\Delta\delta_1$ of IPFC controller with Lead-Lag Controller

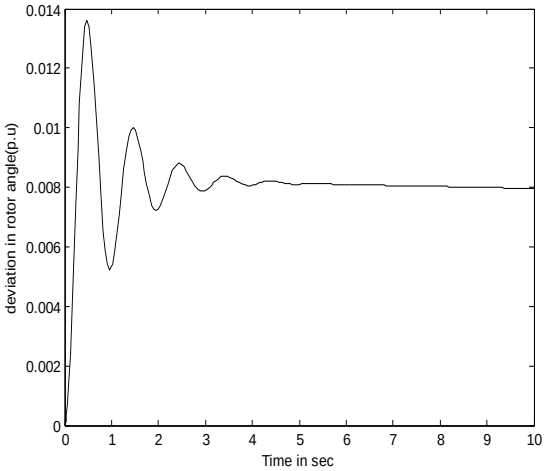

Fig. 12: Response of Rotor angle deviation (Δδ) for δ_1 of IPFC controller with Lead-Lag Controller

ISSN: 2319-5967
ISO 9001:2008 Certified
International Journal of Engineering Science and Innovative Technology (IJESIT)
Volume 3, Issue 1, January 2014

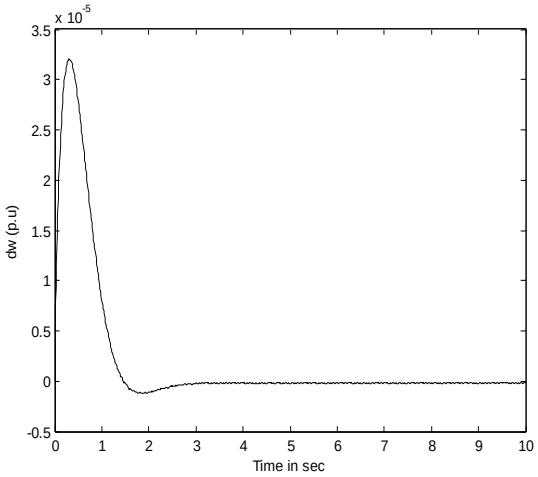

Fig. 13: Response of speed deviation (Δω) for m_2 of IPFC controller with Lead-Lag Controller

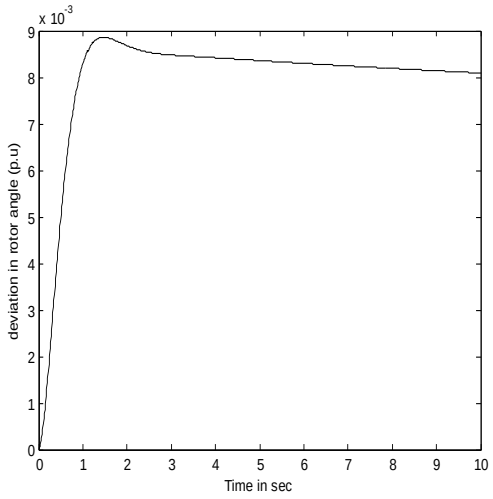

Fig. 14: Response of Rotor angle deviation (Δδ) for m_2 of IPFC controller with Lead-Lag Controller

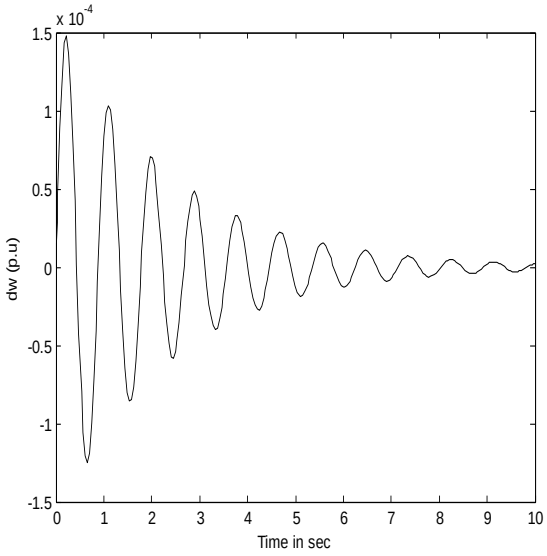

Fig. 15: Response of speed deviation (Δω) for δ_2 of IPFC controller with Lead-Lag Controller

ISSN: 2319-5967
ISO 9001:2008 Certified
International Journal of Engineering Science and Innovative Technology (IJESIT)
Volume 3, Issue 1, January 2014

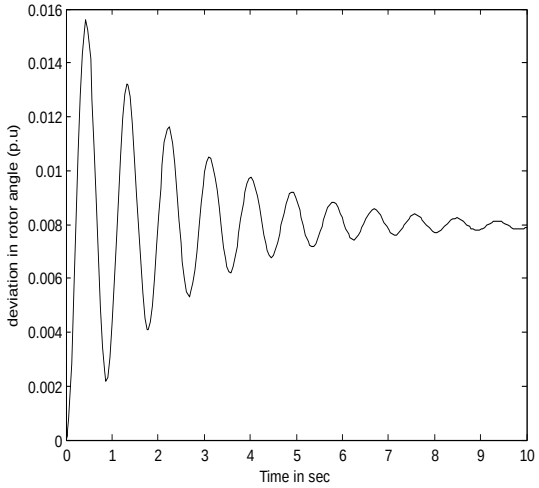

Fig. 16: Response of rotor angle deviation (Δδ) for δ_2 of IPFC controller with Lead-Lag Controller

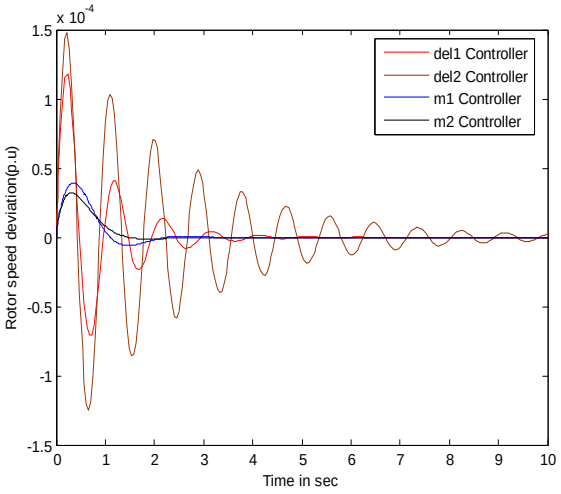

Fig. 17: Response of speed deviation (Δω)

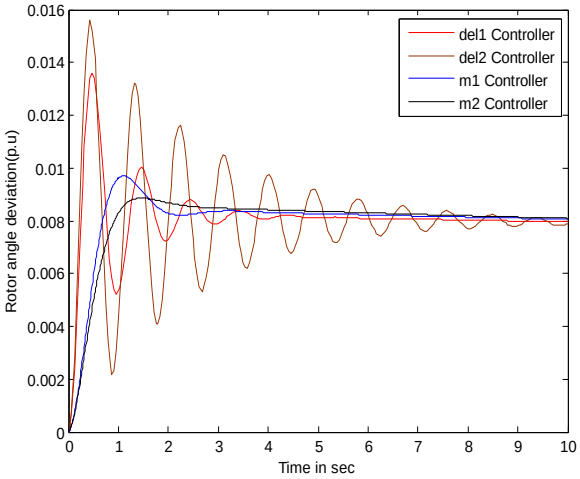

Fig. 18: Response of rotor angle deviation (Δδ)

ISSN: 2319-5967
ISO 9001:2008 Certified
International Journal of Engineering Science and Innovative Technology (IJESIT)
Volume 3, Issue 1, January 2014

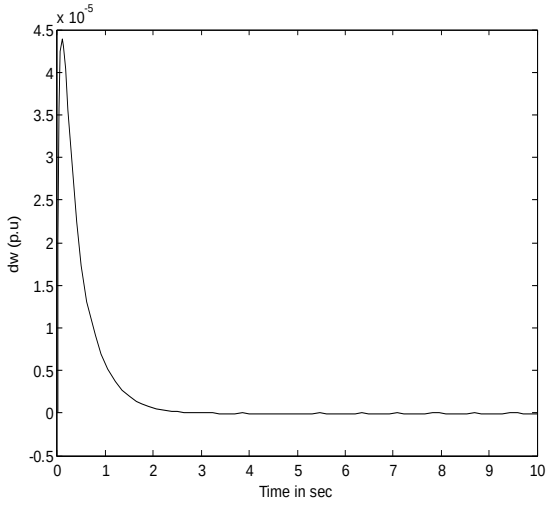

Fig. 19: Response of speed deviation (Δω) with RBFNN Controller (for m_2 IPFC input Parameter)

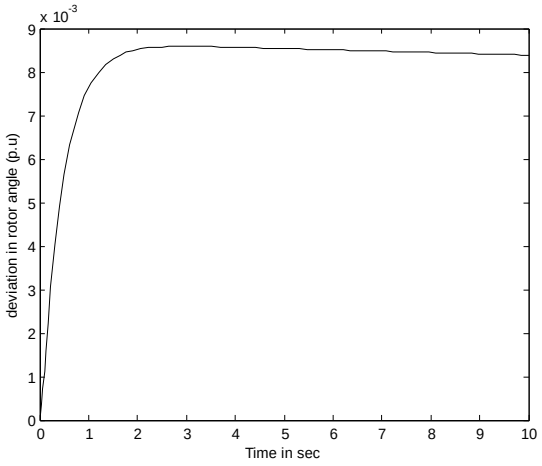

Fig. 20: Response of Rotor angle deviation (Δδ) with RBFNN Controller(for m_2 IPFC input Parameter)

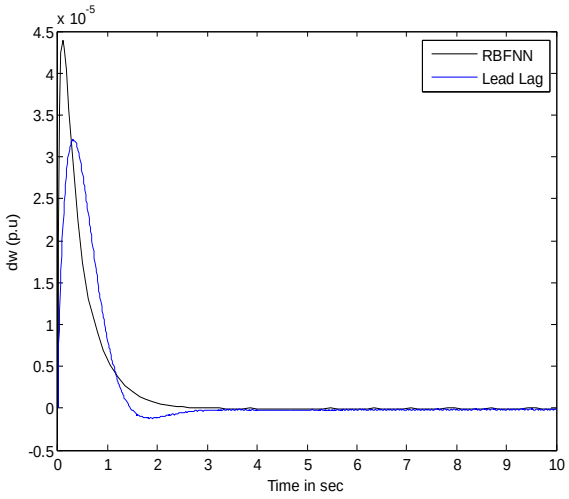

Fig. 21: Response of speed deviation (Δω)

ISSN: 2319-5967
ISO 9001:2008 Certified
International Journal of Engineering Science and Innovative Technology (IJESIT)
Volume 3, Issue 1, January 2014

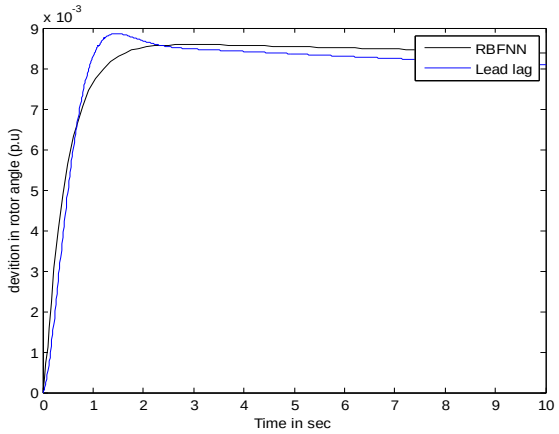

Fig. 22: Response of rotor angle deviation (Δδ)

V. CONCLUSION

Response shown in fig. 7 and 8 are for the circuit shown fig. 6 in the absence of supplementary controller. Response shown in fig. 9-16 are of IPFC used with Lead-Lag controller as supplementary Controller for all the four input (m_1, m_2, δ_1 and δ_2) of IPFC controller. From the response of fig 17 and 18, we observe that m_2 input parameter of IPFC controller gives best among all. Hence, for the next step work, only m_2 parameter is taken into consideration. Response shown in fig. 19 and 20 are of IPFC with RBFNN Controller as supplementary Controller with m_2 input parameter of IPFC controller. From the response of fig. 21 and 22, we observe that the RBFNN gives the better result in comparison to the Lead-Lag Controller. Hence, it is concluded that the RBFNN based IPFC controller gives better damping capability than Lead-Lag based IPFC controller.

APPENDIX

A: Parameter of SMIB System with IPFC

Generator	M=8.0 MJ/MVA	T_{do}'=5.044s	X_d=1.0 pu
	X_q=0.6pu	X_d'=0.3pu	D=0
Reactances	X_s=0.15pu	X_{t1}=0.1pu	X_{t2}=0.1pu
	X_t=0.1pu	X_{L1}=0.5pu	X_{L2}=0.5pu
			X_L=0.5pu
IPFC parameters	m_1=0.15	m_2=0.1	δ_1=28.1^0
			δ_2=-21.1^0
Excitation System		K_A=50	T_A=0.05s
DC link		V_{DC}=2.0pu	C_{DC}=1.0pu

B: Constant for Lead Lag Controller

IPFC Controller Input	Lead-lag controller Parameters			
	K_{DC}	T_w (s)	T_1 (s)	T_2 (s)
m_1	308.1583	13.2799	0.198	0.0195
m_2	300.2638	9.6307	0.1993	0.0198
δ_1	312.4573	9.1681	0.1986	0.0192
δ_2	323.7909	12.2496	0.1931	0.0144

ISSN: 2319-5967
ISO 9001:2008 Certified
International Journal of Engineering Science and Innovative Technology (IJESIT)
Volume 3, Issue 1, January 2014

C: Constant value of PH Model installed with IPFC

Constant	Value	Constant	Value	Constant	Value
K_1	1.0586	K_{pv}	-0.0694	$K_{c\delta 1}$	0.0188
K_2	0.7930	K_{qv}	-0.0226	K_{pm2}	0.5710
K_3	1.9333	K_{vv}	-0.0013	K_{qm2}	0.0041
K_4	0.6549	K_{pm1}	0.5344	K_{vm2}	-0.0926
K_5	-0.1210	K_{qm1}	-0.3035	K_{cm2}	-0.0715
K_6	0.5251	K_{vm1}	0.044	$K_{p\delta 2}$	0.012
K_7	-0.0514	K_{cm1}	0.0327	$K_{q\delta 2}$	0.046
K_8	-0.1070	$K_{p\delta 1}$	0.0403	$K_{v\delta 2}$	-0.017
K_9	0.0007385	$K_{q\delta 1}$	0.0532	$K_{c\delta 2}$	-0.0263
		$K_{v\delta 1}$	-0.0288		

REFERENCES

[1] Narain G. Hingorani, Laszlo Gyugyi, "Understanding FACTS : concept and technology of flexible AC transmission system " , John Wiley & Sons , INC. , Publication , 1999.

[2] Wang, H. F, "Phillips heffron model of power system installed with STATCOM and applications", IEEE Proc. Generation Transmission Distribution, 1999, 145 (2), pp. 521-527.

[3] Jitendra Veeramalla and Sreerama Kumar, "Application of Interline Power Flow Controller for Damping Low Frequency Oscillation in Power System", MEPS 2010, Wroclaw, Poland.

[4] Mr. Subir Datt, Dr. A. K. Roy ," Radial basis function Neural Network based STATCOM controller for Power system dynamic stability enhancement",IEEE Transaction , 2011.